

# Local gravity field continuation for the purpose of in-orbit calibration of GOCE SGG observations

Roland Pail

Institute of Geodesy, Department of Theoretical Geodesy, Graz University of Technology, Steyrergasse 30, A-8010 Graz, Austria

**Abstract.** The use of ground gravity data in well-surveyed areas, continued upward to satellite altitude, is one of the most promising external absolute in-orbit calibration/validation methods for GOCE satellite gravity gradient (SGG) observations. Based on a synthetic gravity test environment – providing in addition to statistical error information also absolute error estimates – several upward continuation methods, e.g. least squares collocation, equivalent source techniques using point masses or area density distributions defined on a spherical surface section, are described, assessed and compared. It turns out that all these strictly local approaches fail to work sufficiently accurate. Consequently, a combined adjustment strategy is proposed, supporting the high-quality gravity field information within the well-surveyed test area with a low-accuracy, but globally defined Earth model. Under quite realistic assumptions the upward continuation is performed with rms errors in the order of 1 mE. The most crucial limiting factor of this method is spectral leakage in the course of an adequate representation of the initial gravity information, which can be overcome by an enlargement of the parameter model in combination with *a priori* filtering of the initial gravity data.

**Key words.** Satellite gravity gradiometry – GOCE – calibration – least squares adjustment

---

## 1 Introduction

The sensors of the satellite gravity field mission GOCE (ESA, 1999) comprise a highly sophisticated measurement system. In particular, GOCE will be the first satellite equipped with a gradiometer. Since an adequate quality assessment of the observation time series is a crucial component for reaching the mission goals, potential calibration/validation procedures have to be identified and investigated. A detailed definition of the terms ‘calibration’ and ‘validation’ can be found in Koop et al. (2001).

There are different approaches for the on-board relative, and the absolute calibration of the GOCE measurement system, which will have to be combined to finally obtain absolutely calibrated physical parameters (ESA, 1999; Koop et al., 2001; Pail, 2002):

- Satellite measuring instrument test before launch.
- On-board calibration (‘relative’), e.g. by means of the Attitude and Orbit Control System (AOCS), i.e. exactly defined thruster firings.
- Comparing gradiometer measurements with the dominant, time-varying gravity gradient terms (e.g. Earth’s flattening term  $J_2$ ).
- Cross-comparison of SST and SGG solutions in the overlapping band of the spectrum.
- Intercomparison between gravity field products from other satellite missions (CHAMP, GRACE, altimetry, ...).
- Comparison with existing (global) gravity field models.
- Use of ground data in well-surveyed areas.

Among those cal/val methods, the use of well-surveyed areas on the Earth’s surface, where the gravity field is known to high accuracy, is one of the most promising approaches (Visser et al., 2000). For this purpose gravity data have to be continued upward to the GOCE satellite altitude of about 250 km and compared with the actual gravity gradient observations. Consequently, two operations have to be performed: an upward continuation of the ground gravity data to the satellite level, and simultaneously a field transformation in terms of a differentiation in order to convert ground gravity information (gravity anomalies, deflections of the vertical) into gravity gradients.

The present paper concentrates on the upward continuation and gravity conversion problem, while some hints on

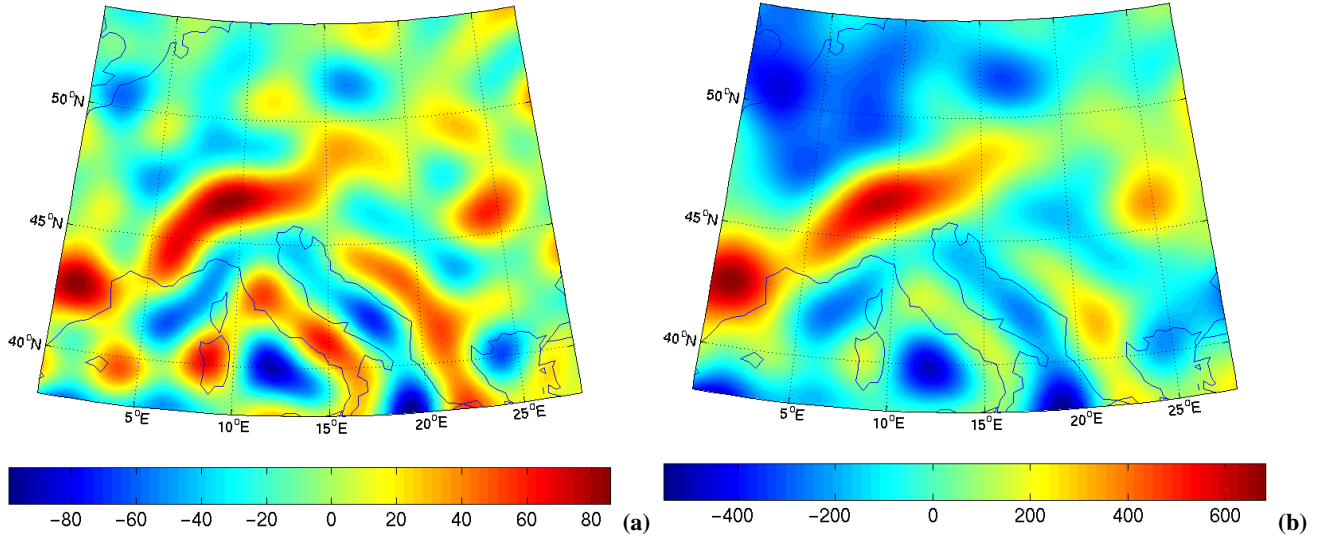


**Fig. 1.** (a) Gravity anomalies [mGal] defined on rough topography and (b) Vertical gravity gradients [mE] at satellite altitude  $h = 250$  km based on synthetic Earth model coefficients in the spectral bandwidth  $0 \leq l \leq 120$ .

the comparison with the actual gravity gradient observations can be found in Pail (2002), Cesare (2002).

The highly accurate gravity information is spatially limited to a few percent of the Earth's surface (e.g. Europe, North America, Japan, parts of Australia, ...). This restriction of the definition domain causes edge effects and leads to omission errors, to a poor representation of the long-wavelength component, and thus results in a poor field continuation quality predominantly of the trend component. Another critical aspect is the reasonable selection of the location, dimension and spectral properties of the test area. Choosing a test region with a very smooth gravity field, and thus a small variance, leads to a very low signal to noise ratio, i.e. the noise component of the gravity sensor should be very clearly detected. On the other hand, in the present context our primary goal is the absolute calibration/validation of the gravity sensor, i.e. the quantitative assessment of its output. Consequently, a high gravity signal, preferably over a wide spectral range, is indispensable to perform this task. In order to be useful for cal/val purposes, the error of the upward continued gravity information must be in the same order as the gradiometer error budget, i.e. about 4 mE ( $1 \text{ mE} = 10^{-9} \text{ s}^{-2}$ ) in the measurement bandwidth of 5 mHz to 100 mHz (Cesare, 2002).

## 2 Test field definition

Since potential systematic deficiencies of the continuation methods are only inadequately reflected by statistical (inner) error estimates, an independent validation of these techniques is required, and one of the most promising approaches is synthetic Earth modelling (Pail, 2000). Based on a previously defined synthetic density distribution in the Earth's

interior, the corresponding potential quantities can be simulated everywhere on and beyond the surface of the synthetic Earth body, thus providing an excellent test environment. Generating synthetic test fields for bounded regions and comparing the continuation results with the known exact solution yields absolute error estimates, reflecting all potential deficiencies of the respective continuation method.

One problem which is common to all methods is a substantially degraded accuracy of the continuation results at the boundaries of the test field. A detailed analysis of these edge effects indicates, that considering gravity gradients at a satellite altitude of about  $h = 250$  km, an edge frame of at least  $2^\circ$  to  $3^\circ$  of the test field is affected, and thus the test field dimensions have to be sufficiently large to ensure a good continuation quality at least in the inner regions.

In the present study, the topography of a European region with a dimension of  $16^\circ \times 28^\circ$ , i.e.  $36^\circ \leq \theta \leq 52^\circ$  in latitude and  $0^\circ \leq \lambda \leq 28^\circ$  in longitude, is used. The corresponding gravity signals, i.e. gravity anomalies defined on the rough topography as the input (Fig. 1a), and vertical gravity gradients (VGG) at 250 km as the 'true' output (Fig. 1b), are based on the synthetic Earth model, which is parameterized in terms of spherical harmonic coefficients complete up to degree/order 300. However, for computational purposes, we restrict ourselves in the sequel to systems of maximum degree and order  $l_{max} = 120$ . The rms of the vertical gravity gradient field at 250 km displayed in Fig. 1b is 199 mE.

## 3 Field continuation techniques: simulations and results

The problem of field continuation is a well-investigated issue, and a variety of methods have been developed. How-

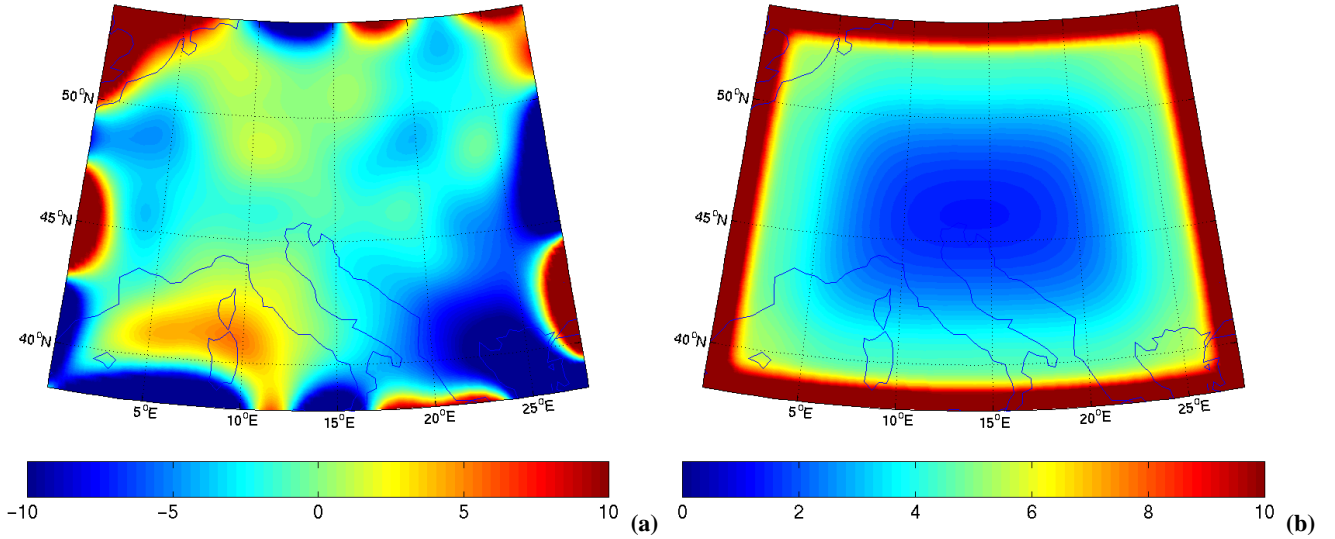


**Fig. 2.** Least squares collocation: **(a)** Vertical gravity gradient deviations [mE] at satellite altitude  $h = 250$  km; initial gravity anomalies composed of spectral components  $13 \leq l \leq 120$  defined on a  $1/4^\circ$  grid, superposed by noise of 1 mGal; local covariance model; **(b)** corresponding error estimates [mE].

ever, in the present context a few quite new aspects arise: the exceptionally large upward continuation distance, combined with a test field of regional size. The field dimension required to produce data along a sufficiently long track is too large to apply techniques based on planar approximation, such as standard Fourier transform or other numerical approximations of Poisson's integral (cf. Heiskanen and Moritz, 1967). On the other hand, the size of well-surveyed areas on the Earth is by far too small to inconsiderately apply standard harmonic base functions with global support such as spherical harmonics. Thus a fair compromise has to be found between the requirement of harmonicity of the base functions, and the bounded definition domain of information available. In the following, several potential solution strategies for this specific upward continuation problem are developed, compared and assessed.

### 3.1 Planar approximations of Poisson's integral and Fourier techniques

The Fourier Transform or similar techniques approximating Poisson's integral are standard methods applied for the purpose of field transformations of local potential fields (e.g., Schwarz et al., 1990; Xia et al., 1993). However, there are a number of requirements to be fulfilled in order to adequately use a planar 2D-Fourier Transform. The most restrictive one certainly is, that the potential quantity has to be given at equidistant grid points on the plane, i.e. in a strict sense neither a curvature of the surface nor a realistic topography are allowed to apply Fourier transform. Several case studies show, that due to the quite large test field dimension required for a reasonable calibration of satellite data, these methods, which are based on planar approximation, are not appropriate

for the present purposes (Pail, 2002).

There are also several pointwise integration techniques over a part of the sphere (e.g. Heiskanen and Moritz, 1967). Haagmans et al. (1993) present the application of a 1D FFT technique on the sphere.

### 3.2 Least squares collocation

Least squares collocation (LSC) is the traditional method for gravity field transformations, being widely used in many geodetic branches, and was also proposed for cal/val purposes. In Visser et al. (2000) error propagation based on the LSC technique was applied to investigate the dependence of the continuation solution on the accuracy, resolution and frequency characteristics of the initial gravity data as well as on the test field size. Arabelos and Tscherning (1996, 1998) investigate gross error rejection strategies and the identification of point or area related errors, as well as the potential identification of systematic errors such as bias and tilt.

In the present study, LSC is applied using alternatively a local two component covariance function model (Rapp, 1979), as well as a global covariance model (Tscherning and Rapp, 1974).

In the first simulation, the strictly local model is applied to a test field which contains only spectral components  $13 \leq l \leq 120$  related to the synthetic Earth model. (Degree  $l = 13$  corresponds to the largest resolvable wavelength with respect to the actual test field dimension.) These gravity signals are superposed by a measuring noise of 1 mGal ( $1 \text{ mGal} = 10^{-5} \text{ m s}^{-2}$ ). Figure 2a illustrates the deviation of the continuation result from the exact vertical gravity gradient at a satellite altitude of  $h = 250$  km. Naturally the largest errors occur at the edges due to the bounded test area.

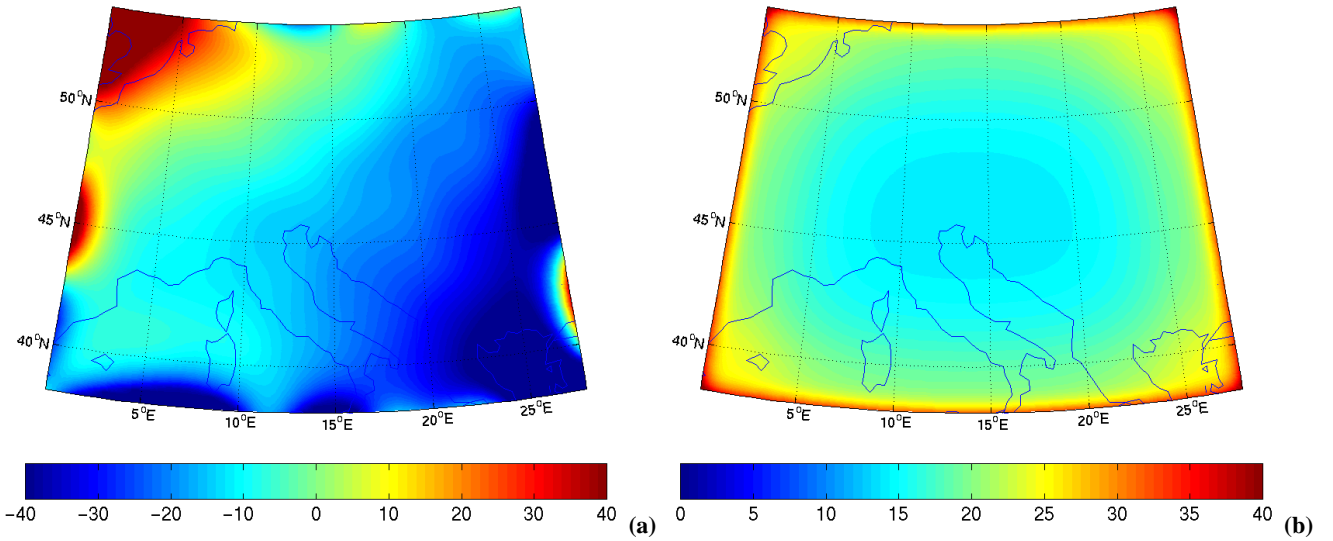


**Fig. 3.** Least squares collocation: **(a)** Vertical gravity gradient deviations [mE] at satellite altitude  $h = 250$  km; initial gravity anomalies composed of spectral components  $0 \leq l \leq 120$  defined on a  $1/4^\circ$  grid, superposed by noise of 1 mGal; global covariance model; **(b)** corresponding error estimates [mE].

Excluding an edge frame of  $3^\circ$ , the rms deviation in the remaining field interior is 3.2 mE. Figure 2b shows the corresponding error estimates, demonstrating that the covariance propagation is quite consistent with the real error behaviour.

In the second case study, which is now based on an input gravity field containing signals with all spectral components  $0 \leq l \leq 120$ , we apply a global covariance model, including the exact degree variances of the synthetic model for the global component. Figures 3a and b show the differences to the exact solution and the corresponding error estimates. Figure 3a plainly illustrates that the dominant error contribution is due to the long wavelength component. The rms of this difference field is substantially enhanced to about 15 mE, which is also consistent with the error covariances displayed in Fig. 3b.

### 3.3 Equivalent source techniques

These methods are based on the *equivalent source principle* of potential theory, stating that there is an infinite number of possible density distributions of different type, such as point masses, area and mass density distributions, dipoles and arbitrary multipoles, which generate identical gravitational effects on the surface, and due to the superposition principle of potential fields even an arbitrary combination of different types of sources fulfils these requirements. The key idea of all equivalent source techniques is to search for such a source distribution, which approximates the available gravity information on the surface in an optimized way. Since the gravitational signals produced by these sources located below the surface are harmonic on and everywhere beyond the surface, they meet the requirements for potential field transformations such as upward continuation.

In the sequel we will concentrate on two representatives of equivalent sources:

- point masses;
- area density distributions.

Concerning the point mass approach, we use a strategy published by Lehmann (1995). An algorithm determining only the magnitudes and the depths of the masses via least squares optimization and previously fixed lateral positions is applied to the solution of the oblique boundary value problem of potential theory. The key concept is a constraint nonlinear optimization of point masses, essentially a nonlinear least squares method of Levenberg-Marquardt type including an active set strategy for linear inequality constraints with respect to the source depth.

The most crucial criterion for a successful application of the point mass technique is the proper choice of the possible depth range where the sources are located, influencing the spectral properties of the potential field on the surface. Numerous simulations reveal that only a multi-step procedure, i.e. a separation of the initial gravity field into at least two components with low pass and high pass spectral content, respectively, and a separate fitting of point mass sets located in two depths bands, results in quite reliable results. However, the best solution achieved shows deviations of about 25 mE from the exact vertical gravity gradient.

As a second equivalent source technique, an area density distribution is used. So far this approach has been developed only for the planar case (Xia et al., 1993), and is extended in Pail (2002) also to the spherical case, proposing an orthonormalized function approach tailored to a local area on the sphere, where spherical harmonics are used as initial base functions (Pail et al., 2001).

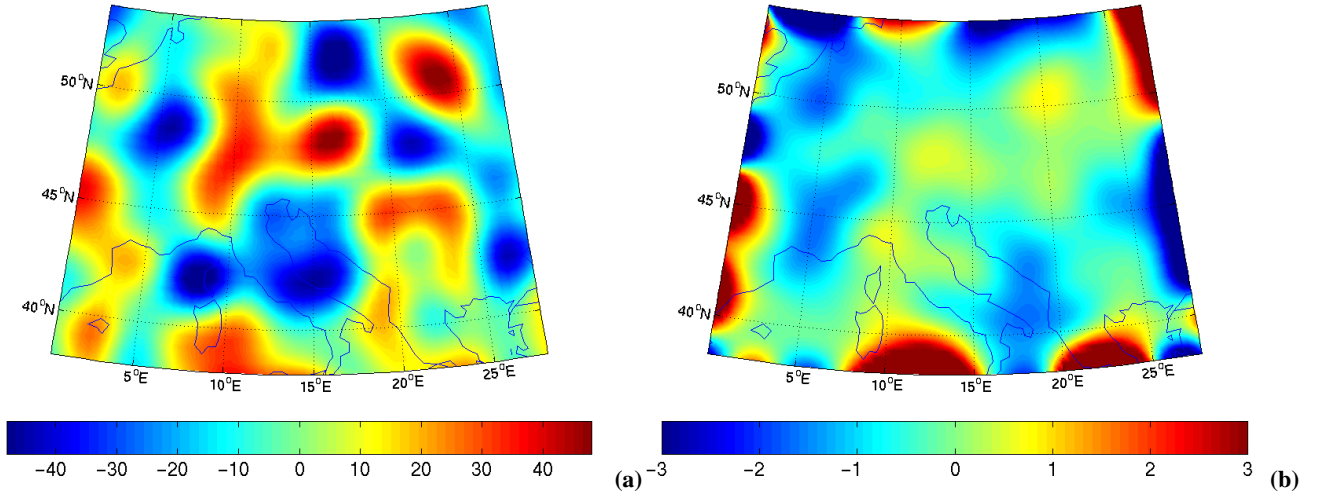


**Fig. 4.** Combined adjustment: Vertical gravity gradient deviations [mE] at satellite altitude 250 km; **(a)** only global gravity model: noise  $1 \sigma_{EGM}$ ; **(b)** global gravity model (noise  $5 \sigma_{EGM}$ ) plus local gravity data defined on a  $1/6^\circ$  grid, superposed by noise of 1 mGal.

Summarizing a variety of simulations performed applying this equivalent source technique, the rms gravity gradient deviations from the exact solution can not be squeezed substantially below 10 mE.

### 3.4 Spherical harmonic expansion by least squares adjustment, supported by global Earth model

From the previous investigations of field continuation methods we have to conclude, that a strictly local solution can not reach the accuracies required, predominantly due to the poor trend field representation and resulting omission errors in the course of the upward continuation. Consequently, it suggests itself to look for an adequate support of the highly accurate, but spatially restricted gravity information in the low degree regions of the spectrum. As a matter of course, the best available gravity information is merged in the recent global Earth models. Although the accuracy of current Earth models such as OSU91a (Rapp et al., 1991) or EGM96 (Lemoine et al., 1998) is too low for cal/val purposes except for the very long wavelengths (Visser et al., 2000), they could be used in combination with the high-accuracy local gravity field information. Thus we intend to benefit from the advantages (and to cope with the insufficiencies) of both components, i.e. the global availability of (rather low accuracy) gravity information of Earth models and the highly accurate (but only regionally available) data within the test area.

In principle, any aforementioned method could be supported by global information. In the following, however, a different approach is proposed. Gathering all the gravity observations performed on the spatially bounded test area in a vector  $\ell$  and the corresponding error covariances in the matrix  $\Sigma_\ell$ , using a standard Gauss-Markov model and applying the best linear uniformly unbiased estimation with respect to

the  $\Sigma_\ell^{-1}$ -norm leads to the normal equation system

$$(A^T \Sigma_\ell^{-1} A) x = A^T \Sigma_\ell^{-1} \ell \quad (1)$$

for the parameter vector  $x$  composed of the harmonic coefficients:  $x = \{\bar{C}_{lm}; \bar{S}_{lm}\}$ . The design matrix  $A$  represents the linear (or linearized) relation between observations  $\ell$  and parameters  $x$ , and thus contains the base functions of the spherical harmonics expansion. However, due to the fact that these spherical harmonics are globally defined, whereas the data are available only on a fraction of the whole globe, the normal equations  $A^T \Sigma_\ell^{-1} A$  are numerically singular.

Introducing the harmonic coefficients related to a global Earth model as a kind of prior information in the vector  $x_o$ , and denoting the corresponding error covariances by  $\Sigma_o$ , the modified normal equation system reads

$$(\Sigma_o^{-1} + A^T \Sigma_\ell^{-1} A) x = \Sigma_o^{-1} x_o + A^T \Sigma_\ell^{-1} \ell, \quad (2)$$

which can be solved for the unknown coefficients  $x$ , provided that the accuracy of the prior information  $\Sigma_o$  is sufficient to make the normal equations  $(\Sigma_o^{-1} + A^T \Sigma_\ell^{-1} A)$  regular.

Applying covariance propagation, the corresponding parameter error covariances are

$$\Sigma_{\hat{x}} = (\Sigma_o^{-1} + A^T \Sigma_\ell^{-1} A)^{-1}. \quad (3)$$

In the present simulation the initial free air gravity field with a spatial extension of  $36^\circ \leq \theta \leq 52^\circ$  by  $0^\circ \leq \lambda \leq 28^\circ$  and defined on the rough topography is composed of all synthetic harmonic coefficients  $0 \leq l \leq 120$ . Since the present approach includes trend field information by means of an a priori known Earth model, it enables to represent also the low frequency component of the test field, and the corresponding coefficients of degrees  $l < 13$  can be introduced both in the test field and in the parameter model.

In the first simulation only the prior information related to the global Earth model is taken into account. Since the

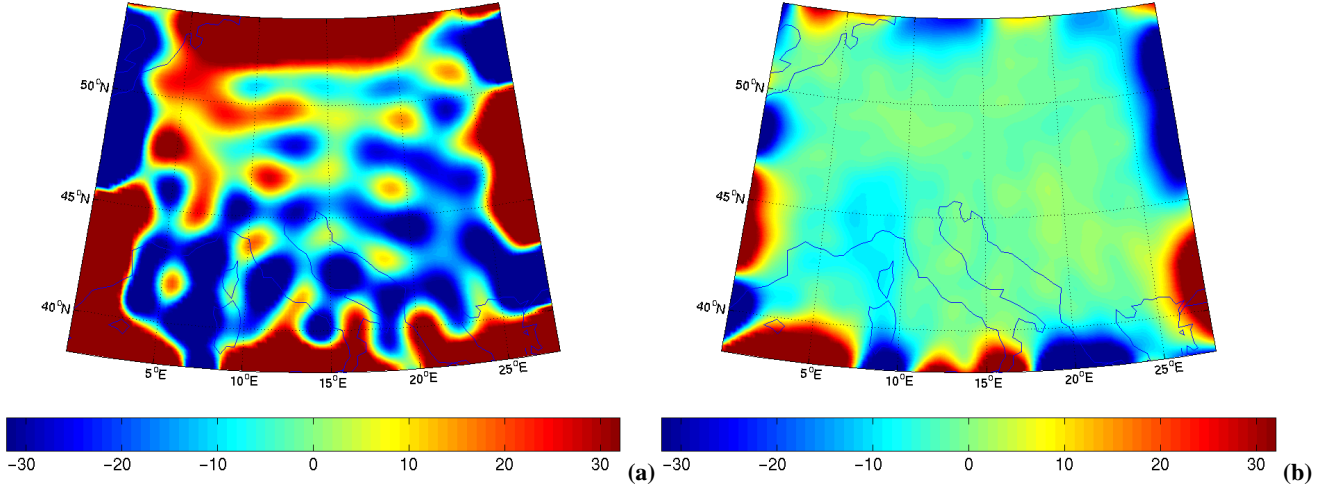


**Fig. 5.** Combined adjustment: Vertical gravity gradient deviations [mE] at satellite altitude 250 km; **(a)** Spectral leakage: global gravity model (noise  $5\sigma_{EGM}$ ) plus local gravity anomaly data composed of spectral components  $0 \leq l \leq 150$  defined on a  $1/4^\circ$  grid, superposed by noise of 1 mGal, parameterization up to  $l_{max} = 120$ ; **(b)** global gravity model (noise  $5\sigma_{EGM}$ ) plus local gravity anomaly data composed of spectral components  $0 \leq l \leq 300$  defined on a  $1/4^\circ$  grid, low pass filter with cut-off wavelength 211 km applied to the gravity field; parameterization up to  $l_{max} = 190$ .

present study is based on a synthetic gravity model, we have to assume that the corresponding coefficients are known to some specified accuracy. Therefore, as prior information  $x_o$  we use the exact coefficients of this model, but each coefficient value is superposed by random noise with a variance  $\sigma_{EGM}^2$  corresponding to the error variances of EGM96. Correspondingly, the error covariances  $\Sigma_o$  are composed of the EGM96 covariances. Naturally in this simplest configuration Eq. (2) reduces to a trivial equation system with the solution  $\hat{x} = x_o$  for the coefficients and  $\Sigma_{\hat{x}} = \Sigma_o$  for the parameter covariances. Figure 4a shows the deviations of the vertical gravity gradient [mE] at satellite altitude  $h = 250$  km from the exact solution. In fact, this figure simply reflects the propagation of the noise component initially applied to the coefficients  $x_o$  onto the VGG at satellite level. The rms deviation of the field in Fig. 4a – neglecting a boundary region of  $3^\circ$  on each side – is about 22.5 mE.

Based on the synthetic gravity model, in the test field region free air anomaly data are simulated on an equiangular grid with a node spacing of  $1/6^\circ \times 1/6^\circ$ , additionally applying a measuring noise of  $\sigma = 1$  mGal to the gravity observations on the grid. Considering the quality of presently available free air gravity data in Europe, this noise amplitude is a very conservative assumption. Additionally, since statistical error estimates tend to be too optimistic, the noise applied to the coefficients  $x_o$  was enhanced to  $5\sigma_{EGM}$ . Figure 4b displays the differences from the exact solution in terms of the VGG [mE] at satellite altitude  $h = 250$  km. Again neglecting an edge frame of  $3^\circ$  for the statistical analysis, the rms deviation of this difference field is approximately 0.63 mE. In order to cross-check the degradation of the continuation quality when having a smaller number of local gravity data available, we recompute the previous simulation with a grid

spacing of  $1/4^\circ$  instead of  $1/6^\circ$ , but with the same a priori global accuracy of  $5\sigma_{EGM}$ . The rms deviation of 0.91 mE is only slightly worse than in the previous case study using a  $1/6^\circ$  grid (Fig. 4b), demonstrating that the major error component is due to the degraded global model accuracy.

In the previous simulations it was implicitly assumed that the initial gravity field is solely composed of signal components up to a specified degree  $l_{max} = 120$ . In practice, it is hopeless to meet such a very strict requirement, because the initial gravity anomaly field can not be perfectly separated into spectral components of low and high degrees  $l$ . This effect of an incomplete parameter model is denoted by spectral leakage, because high frequency signal components are not adequately parameterized and therefore are leaking into the degrees resolved. In order to demonstrate the effect of spectral leakage, a gravity input field based on the synthetic coefficients up to degree  $l_{max} = 150$  was generated on a  $1/4^\circ$  grid, again superposed by a white noise component of 1 mGal. On the contrary, the parameter model applied is composed of a full set of harmonic coefficients only up to degree and order  $l_{max} = 120$ . Figure 5a shows the continuation solution in terms of deviations of the VGG at satellite altitude  $h = 250$  km. The huge rms of 18.7 mE is simply due to the fact, that the initial signals of degrees  $l = 121$  to  $l = 150$  inherent in the gravity anomaly input are inadequately represented by the inconsistent parameter model, and are at least partially mapped to the coefficients of degrees  $l \leq 120$ .

There are two approaches to reduce the spectral leakage problem: Either the parameter model must be sufficiently large to accurately represent the initial gravity signals, or the high frequency components have to be properly eliminated before applying the least squares adjustment. In practice,

**Table 1.** Statistical parameters of the vertical gravity gradient deviations [mE] at satellite altitude 250 km applying different continuation methods to several configurations (confer text), excluding an edge frame of 3°

VGG [mE]	$l_{min}$	$l_{max}$	grid	global	Fig.	min	max	rms
Total field	0	120	1/6°	—	1 (b)	-564.8	408.0	199.00
FFT	13	120	1/6°	—	—	-86.9	46.2	20.24
LSC (local covar.)	13	120	1/4°	—	2 (a)	-10.9	5.4	3.21
LSC (global covar.)	0	120	1/4°	0	3 (a)	-44.8	23.1	15.19
Point masses	13	120	1/6°	—	—	-53.3	72.8	25.73
Area density	13	120	1/6°	—	—	-35.2	25.1	10.62
Comb. adj.: global info. only	0	120	—	1 $\sigma_{EGM}$	4 (a)	-55.7	51.2	22.54
	0	120	—	5 $\sigma_{EGM}$	—	-278.3	256.0	112.70
Comb. adj.: global+ local grid	0	120	1/6°	5 $\sigma_{EGM}$	4 (b)	-1.8	0.8	0.63
	0	120	1/12°	1 $\sigma_{EGM}$	—	-1.0	0.4	0.26
	0	120	1/12°	5 $\sigma_{EGM}$	—	-3.1	1.2	0.78
	0	120	1/4°	5 $\sigma_{EGM}$	—	-3.4	1.8	0.91
	0	120	irreg.*	5 $\sigma_{EGM}$	—	-3.5	1.4	0.98
Comb. adj.: leakage	0	150/120*	1/4°	5 $\sigma_{EGM}$	5 (a)	-70.0	70.8	18.70
Comb. adj.: leakage+filter	0	150/120*	1/4°	5 $\sigma_{EGM}$	—	-28.2	24.2	6.95
Comb. adj.: global+local grid	0	170	1/4°	—	—	-3.5	2.1	1.03
Comb. adj.: leakage+filter	0	300/170*	1/4°	5 $\sigma_{EGM}$	—	-14.4	7.6	3.55
	0	300/190*	1/4°	5 $\sigma_{EGM}$	5 (b)	-10.4	4.6	2.65

\* locations randomly distributed, with a mean distance of 1/4°

\* max. degree of signal / of parameterization

a combination of both approaches suggests itself. Consequently, in the next simulation a FFT low pass filtering procedure was applied to the test field containing spectral components up to a maximum degree  $l_{max} = 150$ , in order to reduce the high pass component. Since degree  $l = 120$  corresponds to a spatial wavelength of about 334 km, this value is used as the filter cut-off wavelength. The VGG rms error is reduced from initially 18.7 mE for the unfiltered solution to less than 7 mE, but this gain in accuracy does not suffice for practical calibration/validation purposes, and therefore the additional enhancement of the parameter model has to be envisaged.

Due to the fact that the base functions in Eq. (2) are correlated, in general the normal equation system is full. Therefore, its solution requires enhanced computational capabilities. A parallel computing strategy is applied to solve these large and generally full normal equation systems. In the framework of the project ‘Scientific Supercomputing’ at Graz University of Technology, a parallel computing system based on the Beowulf concept is operable. At the present stage, it is composed of 24 dual-processor (866 MHz) PCs, each with 1 GB RAM and 18 GB local hard disk (Plank, 2001).

In the last case study, such a large system shall be analyzed. The initial gravity signal contains spectral components up to degree  $l_{max} = 300$ , and the parameter model was enlarged up to degree  $l_{max} = 190$ , leading to a normal equation system of more than 665 million independent elements, corresponding to a memory requirement of about 5.5 GB. A prior low pass filtering of the initial gravity field with a filter cut-off wavelength of 211 km (corresponding to degree

$l_{max} = 190$ ) was applied, and a combined adjustment was computed, again assuming an accuracy of the global model of  $5 \sigma_{EGM}$ . The rms deviations of the resulting difference field displayed in Fig. 5b are reduced to 2.65 mE. This considerable gain of accuracy proves, that in practice the strategy to enlarge the parameter model, together with a prior filtering of the initial gravity field, is well-suited to reduce the leakage problem.

### 3.5 Summary and discussion

Table 1 summarizes the major statistical properties of the vertical gravity gradient deviations at a satellite altitude of  $h = 250$  km related to a variety of case studies, some of them explicitly described in the previous Sects. 3.1 to 3.4, reducing edge effects by excluding an edge frame of 3°.

From these results it can be concluded that the combined adjustment method is well suited to solve the continuation problem, while all the other strictly local methods discussed in the Sects. 3.1 to 3.3 fail in an adequate representation and thus in a correct continuation particularly of the low frequency component. Consequently, the introduction of some kind of trend field information is indispensable to solve the continuation problem.

In Sect. 3.4 it was pointed out, that in practice the most crucial problem will be spectral leakage, because the initial gravity anomaly field can not be perfectly separated into spectral components of low and high degrees  $l$ . In fact this problem is of aporetic nature, because if such a perfect harmonic representation would be possible, the whole problem could be solved easily, due to the fact that in this case also

a correct field continuation and field transformation without energy shifts among the spectral components could be performed. The underlying reason for this argumentation is again the bounded definition domain of the gravity data. However, this problem can be considerably reduced by extending the parameter model to sufficiently large degrees  $l_{max}$  in order to properly represent the initial gravity information, in combination with an a priori low pass filtering of the input gravity signal.

At this point it should be emphasized that these simulations are based on some very conservative assumptions especially concerning the accuracy of the global information and the resolution of the ground gravity data. Even in this case the resulting rms deviations are below the 3 mE-level. However, since the solution strategy applied is a kind of weighted merging of a quite inaccurate global gravity information and the high-accuracy local gravity data, the effects of the relative contributions of these two components – with special concern to the influences on the numerical stability of the corresponding normal equations – will require further analysis in the case of larger systems.

An extended version of this paper can be found in Pail (2002).

*Acknowledgements.* This study was performed in the course of the GOCE project “From Eötvös to mGal+”, funded by the European Space Agency (ESA) under contract no. 14287/00/NL/DC.

## References

- Arabelos, D. and Tscherning, C. C.: Support of Spaceborne Gravimetry Data Reduction by Ground Based Data, ESA-Project CIGAR IV, WP 3, Final Report, 95–156, 1996.
- Arabelos, D. and Tscherning, C. C.: Calibration of satellite gradiometer data aided by ground gravity data, *J. Geod.*, 72, 617–625, 1998.
- Cesare: Performance requirements and budgets for the gradiometric mission, Technical Note, GOC-TN-AI-0027, Alenia Spazio, Turin, Italy, 2002.
- ESA: Gravity Field and Steady-State Ocean Circulation Mission. Reports for mission selection, The four candidate Earth explorer core missions, SP-1233(1), European Space Agency, 1999.
- Haagmans, R., de Min, E., and van Gelderen, M.: Fast evaluation of convolution integrals on the sphere using 1D FFT, and a comparison with existing methods for Stokes’ integral, *Manuscripta Geodaetica*, 18, 5, 227–241, 1993.
- Heiskanen, W. A. and Moritz, H.: *Physical Geodesy*, W. H. Freeman and Company, San Francisco, London, 1967.
- Koop, R., Visser, P., and Tscherning, C. C.: Aspects of GOCE calibration, in: Proc. International GOCE User Workshop, April 2001, ESA/ESTEC, WPP-188, 51–56, European Space Agency, Noordwijk, 2001.
- Lehmann, R.: Gravity field approximation using point masses in free depths, *The International Association of Geodesy (IAG), Section IV Bulletin*, no. 1, 129–140, 1995.
- Lemoine, F. G., Kenyon, S. C., Factor, J. K., Trimmer, R. G., Pavlis, N. K., Chinn, D. S., Cox, C. M., Klosko, S. M., Luthcke, S. B., Torrence, M. H., Wang, Y. M., Williamson, R. G., Pavlis, E. C., Rapp, R. H., and Olson, T. R.: The Development of the Joint NASE GSFC and the National Imagery and Mapping Agency (NIMA) Geopotential Model EGM96, National Aeronautics and Space Administration, Goddard Space Flight Center, Greenbelt, Maryland, 1998.
- Pail, R.: Synthetic Global Gravity Model for Planetary Bodies and Applications in Satellite Gravity Gradiometry, Dissertation, *Mitteil. geodät. Inst. TU Graz*, 85, 135 p., Graz University of Technology, 2000.
- Pail, R.: In-orbit calibration and local gravity field continuation problem, ESA-Project “From Eötvös to mGal+”, ESA/ESTEC Contract 14287/00/NL/DC, Final Report, WP 1, 9-112, European Space Agency, Noordwijk. ([www-geomatics.tu-graz.ac.at/mggi/research/e2mgp/e2mgp.htm](http://www-geomatics.tu-graz.ac.at/mggi/research/e2mgp/e2mgp.htm)), 2002.
- Pail, R., Plank, G., and Schuh, W.-D.: Spatially restricted data distribution on the sphere: the method of orthonormalized functions and applications, *J. Geod.*, 75, 44–56, 2001.
- Plank, G.: Implementation of the PCGMA-package on massive parallel systems, ESA project ‘From Eötvös to mGal+’, ESA/ESTEC Contract 14287/00/NL/DC, Final Report, WP 3, 183-216, European Space Agency, Noordwijk, 2001.
- Rapp, R. H.: Potential coefficient and anomaly degree variance modelling revisited, *OSU Rep. no. 2*, The Ohio State Univ., Columbus, Ohio, 1979.
- Rapp, R., Wang, Y., and Pavlis, N.: The Ohio state 1991 geopotential and sea surface topography harmonic coefficient models, *OSU Report 410*, Department of Geodetic Science and Surveying, The Ohio State University, Columbus, Ohio, 1991.
- Schwarz, K. P., Sideris, M. G., and Forsberg, R.: The use of FFT techniques in physical geodesy, *Geophys. J. Int.*, 100, 485–514, 1990.
- Tscherning, C. C. and Rapp, R. H.: Closed covariance expressions for gravity anomalies, geoid undulations, and deflections of the vertical implied by anomaly degree variance models, *OSU Rep. no. 208*, Department of the Geodetic Science and Surveying, The Ohio State Univ., Columbus, Ohio, 1974.
- Visser, P., Koop, R., and Klees, R.: Scientific data production quality assessment, ESA-Project “From Eötvös to mGal+”, Final Report, WP 4.1, 157–176, 2000.
- Xia, J., Sprowl, D. R., and Adkins-Heljeson, D.: Correction of topographic distortions in potential-field data: A fast and accurate approach, *Geophysics*, 58, 515–523, 1993.